



HAL
open science

Defective type I interferon immunity is associated with increasing COVID-19 severity

Nikaï Smith, Célin Possémé, Vincent Bondet, Jamie Sugrue, Liam Townsend, Bruno Charbit, Vincent Rouilly, Violaine Saint-André, Tom Dott, Andre Rodriguez Pozo, et al.

► **To cite this version:**

Nikaï Smith, Célin Possémé, Vincent Bondet, Jamie Sugrue, Liam Townsend, et al.. Defective type I interferon immunity is associated with increasing COVID-19 severity. 2022. pasteur-03699367

HAL Id: pasteur-03699367

<https://pasteur.hal.science/pasteur-03699367>

Preprint submitted on 20 Jun 2022

HAL is a multi-disciplinary open access archive for the deposit and dissemination of scientific research documents, whether they are published or not. The documents may come from teaching and research institutions in France or abroad, or from public or private research centers.

L'archive ouverte pluridisciplinaire **HAL**, est destinée au dépôt et à la diffusion de documents scientifiques de niveau recherche, publiés ou non, émanant des établissements d'enseignement et de recherche français ou étrangers, des laboratoires publics ou privés.



Distributed under a Creative Commons Attribution 4.0 International License

Defective type I interferon immunity is associated with increasing COVID-19 severity

Darragh Duffy (✉ darragh.duffy@pasteur.fr)

Translational Immunology Lab, Institut Pasteur <https://orcid.org/0000-0002-8875-2308>

Nikaïa SMITH

Translational Immunology Lab, Institut Pasteur <https://orcid.org/0000-0002-0202-612X>

Céline Possémé

Translational Immunology Lab, Institut Pasteur

Vincent Bondet

Institut Pasteur Paris <https://orcid.org/0000-0002-6534-0984>

Jamie Sugrue

Trinity Biomedical Sciences Institute, Trinity College <https://orcid.org/0000-0001-7270-3838>

Liam Townsend

Trinity Biomedical Sciences Institute, Trinity College <https://orcid.org/0000-0002-7089-0665>

Bruno Charbit

Institut Pasteur <https://orcid.org/0000-0002-5478-482X>

Vincent Rouilly

Datactix

Violaine Saint-André

Institut Pasteur

Tom Dott

Institut Pasteur

Andre Rodriguez Pozo

Translational Immunology Lab, Institut Pasteur

Nader Yatim

Institut Pasteur

Olivier Schwartz

Institut Pasteur <https://orcid.org/0000-0002-0729-1475>

Minerva Cervantes-Gonzales

AP-HP, Hôpital Bichat

Jade Ghosn

Department of Infectious and Tropical Diseases, Assistance Publique-Hôpitaux de Paris, Bichat-Claude Bernard University Hospital, Paris, France; Infections Antimicrobials Modelling Evolution

Paul Bastard

Imagine Institute

Jean-Laurent Casanova

Imagine Institute

Tali-Anne Szwebel

Institut Cochin, APHP

Benjamin Terrier

Medical Intensive Care Unit, Assistance Publique-Hôpitaux de Paris Cochin University Hospital, Paris, France.

Niall Conlon

Department of Immunology, St James's Hospital

Cliona O'Farrelly

Trinity College Dublin

Cliona Ni Cheallaigh

Trinity College, Dublin

Nollaig Bourke

Trinity College Dublin

Article

Keywords:

Posted Date: June 16th, 2022

DOI: <https://doi.org/10.21203/rs.3.rs-1685544/v1>

License:  This work is licensed under a Creative Commons Attribution 4.0 International License.

[Read Full License](#)

Defective type I interferon immunity is associated with increasing COVID-19 severity

Nikaïa Smith*¹, Céline Possémé*¹, Vincent Bondet*¹, Jamie Sugrue², Liam Townsend^{3,4}, Bruno Charbit⁵, Vincent Rouilly⁶, Violaine Saint-André^{1,7}, Tom Dott⁵, Andre Rodriguez Pozo¹, Nader Yatim¹, Olivier Schwartz⁸, Minerva Cervantes-Gonzales^{9,10,11}, Jade Ghosn^{9,11}, Paul Bastard^{12,13,14,15}, Jean Laurent Casanova^{12,13,14,15,16}, Tali-Anne Szwebel¹⁷, Benjamin Terrier¹⁷, Niall Conlon^{18,19}, Cliona O'Farrelly^{2,19}, Clíona Ní Cheallaigh^{3,4}, Nollaig M Bourke²⁰, Darragh Duffy^{#1,5}

1 Institut Pasteur, Université Paris Cité, Translational Immunology Unit, Paris, France

2 School of Biochemistry and Medicine, Trinity Biomedical Sciences Institute, Trinity College Dublin, Ireland

3 Discipline of Clinical Medicine, School of Medicine, Trinity Translational Medicine Institute, Trinity College Dublin, Dublin, Ireland

4 Department of Infectious Diseases, St James's Hospital, Dublin, Ireland

5 Institut Pasteur, Université Paris Cité, CBUTechS, Center for Translational Research, Paris, France

6 Datactix, Bordeaux, France

7 Institut Pasteur, Hub de Bioinformatique et Biostatistique – Département Biologie Computationnelle, Paris, France

8 Institut Pasteur, Virus and Immunity, Department of Virology, Paris, France

9 AP-HP, Hôpital Bichat, Infectious and Tropical Diseases Department, Paris, France

10 AP-HP, Hôpital Bichat, Infectious and Tropical Diseases Department, Paris, France

11 Université de Paris, INSERM, IAME UMR 1137, Paris, France

12 Department of Pediatrics, Necker Hospital for Sick Children, AP-HP, Paris, France.

13 Laboratory of Human Genetics of Infectious Diseases, Necker Branch, INSERM U1163, Necker Hospital for Sick Children, Paris, France.

14 Université Paris Cité, Imagine Institute, Paris, France.

15 St. Giles Laboratory of Human Genetics of Infectious Diseases, Rockefeller Branch, The Rockefeller University, New York, NY, USA.

16 Howard Hughes Medical Institute, New York, NY, USA

17 Institut Cochin, APHP, Paris, France

18 Department of Immunology, St James's Hospital, Dublin, Ireland

19 Discipline of Immunology, School of Medicine, Trinity College Dublin, Ireland

20 Discipline of Medical Gerontology, School of Medicine, Trinity Translational Medicine Institute, Trinity College Dublin, Ireland

* Equal contributions

Corresponding author

Abstract

Host immunity to infection with SARS-CoV-2 is highly variable, dictating diverse clinical outcomes ranging from asymptomatic to severe disease and death. We previously reported that reduced blood type I interferon (IFN-I) in severe COVID-19 patients preceded clinical worsening. These results were supported by studies which identified genetic mutations in *loci* of the TLR3- or TLR7-dependent IFN-I pathways, or autoantibodies neutralizing IFN α or IFN ω , as major risk factors for development of severe and critical COVID-19 pneumonia. Here, we analyzed a range of IFN-I associated responses in patient cohorts with different severities of COVID-19, showing that baseline plasma IFN α measures differed significantly according to the immunoassay used, as well as timing of sampling, the IFN α subtype measured, and the presence of autoantibodies. We then compared immune responses induced by *ex vivo* stimulation between non-hospitalized moderate cases (n=27) and hospitalized (n=17) adult patients that required oxygen supplementation. This showed a consistently reduced induction of IFN-I proteins in hospitalized COVID-19 patients upon stimulation, that was not associated with detectable neutralizing autoantibodies against IFN α or IFN ω . We confirmed the poor induction of IFN-I in an independent patient cohort (n=33), and showed it was more pronounced with severe disease. Intracellular proteomic analysis showed that while monocyte numbers were increased in hospitalized COVID-19 patients, they did not secrete IFN-I in response to stimulation. This was further confirmed by *ex vivo* whole blood stimulation with IFN-I which induced a transcriptomic response associated with inflammation in hospitalized COVID-19 patients, that was not seen in controls or non-hospitalized moderate cases. These results may explain the dichotomy of the poor clinical response to IFN-I based treatments in late stage COVID-19, despite the critical importance of IFN-I in early acute infection. An improved understanding of such variable responses to treatment may help to identify potential alternative therapeutic strategies.

Introduction

Type I interferons (IFN-I) are key components of innate anti-viral immune activity and therefore a target for viral interference strategies ¹. We previously reported impaired IFN-I responses in severe COVID-19 patients that preceded clinical worsening ². These observations were further supported by studies led by the COVID Human Genetics Effort (www.covidhge.com) which identified mutations in *loci* that govern Toll-Like Receptor (TLR)3- and interferon regulatory factor (IRF)7-dependent IFN-I immunity ³, or autoantibodies

against IFN α , IFN ω or IFN β ^{4, 5}, as major risk factors for development of severe COVID associated pneumonia ⁶. Additional genetic studies have identified TLR7 pathway to also be critical for host immunity to infection with SARS-CoV-2 ⁷. Despite this key role in early immunity to SARS-CoV-2 infection, the use of exogenous IFN-I as a treatment for COVID-19 ^{8,9} has not improved clinical outcomes. However, in these studies, IFN-I was given late in the disease course and patient were not stratified ^{8,9}. The dichotomous IFN-I activity likely reflects the two-step nature of IFN-I responses in COVID-19 pathogenesis ¹⁰, with the first step characterised by high IFN-I activity required for viral suppression by innate anti-viral immunity. If step 1 is ineffective, for reasons described above, and the virus is not cleared, viral dissemination, hyper-inflammation and compromised adaptive immunity occur, followed by pneumonia and death in a significant proportion of patients.

Despite the clear importance of IFN-I in early innate immunity against SARS-CoV-2 infection, previous studies have reported increased levels of IFNs ¹¹ and interferon-stimulated genes (ISGs) ¹² as biomarkers for mortality. These differences in reporting the precise role of IFN-I may be due to differences in disease kinetics ^{13,14}, patient populations ¹⁵, reporting of IFN protein data *versus* interferon stimulated gene (ISG) expression ^{16,17}, multiple IFN-I subtypes ^{18,19}, the anatomical site studied ^{20,21} or even technical differences in the assays employed ²². Indeed, IFN α protein has been notoriously challenging to measure, leading to the use of ISGs as a proxy readout for IFN signaling. We previously developed a digital ELISA that permits the ultrasensitive detection of all IFN α subtypes ²³, or specifically the IFN α 2 subtype ²⁴. Notably, in blood samples from multiple autoimmune cohorts with clinically known IFN driven pathology, IFN α protein levels were below limits of detection of conventional ELISA/Luminex assays but were quantifiable using our approach ²³. This highlights the importance of employing sufficiently sensitive and qualified immunoassays when studying type I IFN directly from patient samples. Furthermore, while plasma IFN levels may reflect *in vivo* anti-viral activity at the moment of patient sampling, it does not necessarily inform on the ability of patients' cells to respond to a viral encounter. This requires the use of functional immune assays with standardized approaches that minimize technical variability ²⁵, particularly important in heterogenous patient populations.

To better clarify how different IFN-I measures might be used to understand COVID-19 pathogenesis, we compared cases of moderate COVID-19 with patients hospitalized for severe disease across different countries and clinical centers. For baseline responses, we characterized IFN α proteins with highly sensitive assays recognizing either specifically IFN α 2 or all 13 alpha subtypes, as well as IFN function, ISGs, and autoantibodies neutralizing IFN-I. In a subgroup

of these patients, we stimulated whole blood with relevant viral agonists to further assess the functional capacity of their immune system to respond to external perturbation. We highlight the importance of using sufficiently sensitive and qualified assays for measuring IFN-I proteins, and report defective IFN-I induction that is consistent in all hospitalized COVID-19 patients. The defective IFN-I induction in response to these stimuli was not due to autoantibodies potentially masking the protein, except in one patient. We also demonstrate that *ex vivo* IFN-I stimulation of blood from hospitalized patients induces a non-canonical inflammatory response, perhaps explaining the poor clinical outcome to IFN-I based treatments previously reported. Our study highlights the importance of this crucial anti-viral immune response in host protection against SARS-CoV-2 infection, supports strategies for earlier more targeted therapeutic intervention and highlights the importance of using consistent technical approaches for investigation of IFN-Is in human cohort studies.

Materials and Methods

Patient cohorts

Clinical cohorts are summarised in Table S1. Healthy controls and patients acutely infected with SARS-CoV-2 virus were previously described (Table S2) or recruited as inpatients or as outpatients following receipt of a positive SARS-CoV-2 nasopharyngeal swab PCR test at St James's Hospital (SJH) in Dublin, Ireland (n=138) (Table S4) from March-June, 2020. Ethical approval was obtained for the study from the Tallaght University Hospital (TUH)/St James's Hospital (SJH) Joint Research Ethics Committee (reference REC 2020-03). Severity grades were based on admission and supplemental oxygen requirements at the time of sampling. Moderate patients did not require hospitalization at any timepoint. Hospitalized patients requiring supplemental oxygen via nasal cannula (maximal supplemental oxygen flow of up to 6L/min) were considered severe, with critical disease classified as requiring more than 6L of oxygen per minute, either delivered via high-flow nasal oxygen (Airvo) or a venturi mask, a clinical definition previously defined^{3,4}. Additional hospitalized patients (severe and critical cases) were also recruited for cellular and functional assays (Tables S3 and S5) from Hopital Cochin and Hopital Bichat, Paris under clinical study protocols in the setting of the local RADIPEM biological samples collection, derived from samples collected in routine care as previously described², or from the INSERM-sponsored French COVID-19 clinical study (NCT04262921). Biological collection and informed consent were approved by the Direction de la Recherche Clinique et Innovation and the French Ministry of Research (no. 2019-3677,

2020-A00256-33). The studies conformed to the principles outlined in the Declaration of Helsinki, and received approval by the appropriate Institutional Review Boards (Cochin-Port Royal Hospital, Paris; no AAA-2020-08018 and Comité de protection des personnes Ile de France VI; no 2020-A00256-33). Plasma samples were obtained from COVID-19 patients (n=342) for cytokine analysis and for autoantibody analysis (n=212), and whole blood for immune stimulations (n=77) and cellular phenotyping (n=31) from subgroups. Written informed consent was obtained from all study participants. Healthy controls (n=61) were asymptomatic adults, matched with individuals with COVID-19 on age (± 5 years), who had a negative SARS-CoV-2 RT-PCR test at the time of inclusion.

Cytokine assays

Prior to protein analysis, plasma and TruCulture supernatants were treated in a P3 laboratory for viral decontamination using a protocol previously described for SARS-CoV²⁶ which we validated for SARS-CoV-2. Briefly, samples were treated with TRITON X100 (TX100) 1% (v/v) for 2hrs at RT. IFN α 2 and IFN β proteins were quantified by Simoa assays developed with Quanterix Homebrew kits as previously described². Multiple IFN α protein subtypes (named Multi IFN α subtypes) were measured with an IFN α multi-subtype prototype assay (Quanterix), using IFN α 17 (PBL Assay Science) as a reference recombinant standard. For the IFN α 2 assay, the BMS216C (eBioscience) antibody clone was used as a capture antibody after coating on paramagnetic beads (0.3mg/mL), and the BMS216BK already biotinylated antibody clone was used as the detector at a concentration of 0.3 μ g/mL. The SBG revelation enzyme concentration was 150pM. Recombinant IFN α 2c (eBioscience) was used as calibrator. The SBG revelation enzyme concentration was 150pM. Recombinant protein (PBL Assay Science) was used to quantify IFN γ concentrations. For the IFN β assay, the 710322-9 IgG1, kappa, mouse monoclonal antibody (PBL Assay Science) was used as a capture antibody after coating on paramagnetic beads (0.3 mg/mL), and the 710323-9 IgG1, kappa, mouse monoclonal antibody (PBL Assay Science) was biotinylated (biotin/antibody ratio = 40/1) and used as the detector antibody at a concentration of 1 μ g/mL. The SBG revelation enzyme concentration was 50pM. Recombinant protein (PBL Assay Science) was used to quantify IFN β concentrations. The limit of detection (LOD) of these assays were 0.6-2 fg/mL for IFN α 2, 0.6 pg/mL for IFN β , 0.6fg/mL for the IFN α multi-subtype. An additional 44 cytokines and chemokines, including IFN α 2 were measured in plasma and TruCulture supernatants with a commercial Luminex multi-analyte assay (Biotechne, R&D systems).

Functional Immune Assays

For whole blood stimulation, TruCulture tubes (Myriad RBM) containing Poly I:C (20 μ g/ml), R848 (1 μ M), LPS-EB (ultrapure) (10ng/ml) (all Invivogen), and IFN- α 2 (Intron A, Merck) dissolved in 2 mL of buffered media were batch produced as previously described²⁷. Tubes were thawed at room temperature and 1 mL of fresh blood was distributed into each tube within 15 min of collection. Tubes were mixed by inverting them and incubated at 37°C for 22 hours in a dry block incubator. After the incubation time, a valve was manually inserted into the tube to separate the supernatant from the cells. Supernatant was collected, aliquoted and immediately stored at -80°C for protein secretion analysis. Cell pellets of the TruCulture tubes were resuspended in 2ml of Trizol LS (Sigma) and tubes were vortexed for 2 min at 2000 rpm and stored at -80°C for gene expression analysis.

Flow Cytometry

Whole blood was retrieved and incubated in PBS containing 2% foetal calf serum and 2 mM EDTA (FACS buffer) for 10 minutes at 37°C. After centrifugation, supernatant was removed, and 1x RBC lysis buffer (Biolegend) was added for 15 min at room temperature. Cells were washed in PBS and then incubated with a viability stain (Zombie-Aqua, BioLegend) for 10 min at 4°C. After washing, the cells were resuspended in FACS buffer and stained with an extracellular mix containing the antibodies shown in Table S6. For intracellular staining, Fixation/Permeabilization Solution Kit (BD Cytfix/Cytoperm) was used according to the manufacturer's protocol. Briefly, the cells were fixed for 10 min at 4°C with 100 μ l of the Fixation/Permeabilization solution and then washed and stained in 100 μ l of the BD Perm/Wash Buffer containing the intracellular mix of antibodies for 1 hour at 4°C. Data acquisition was performed on a FACS LSR flow cytometer using FACSDiva software (BD Biosciences, San Jose, CA). FlowJo software (Treestar, Ashland, OR) was used to analyze data.

Nanostring gene expression arrays

Total RNA was extracted from Trizol-stabilized cell pellets using NucleoSpin 96 miRNA kit (Macherey-Nagel). RNA concentrations were measured using Quantifluor RNA system kit (Promega) and RNA integrity numbers were determined using the Agilent RNA 6000 Nano kit (Agilent Technologies). Total RNA samples were analyzed using the Human Host Response panel profiling 800 immunology and host response related human genes (Nanostring). Gene expression data were normalized as previously described²⁸.

Autoantibody measurement

Recombinant human (rh)IFN α 2 (Miltenyi Biotec, reference number 130-108-984) or rhIFN ω (Merck, reference number SRP3061), were first biotinylated with EZ-Link Sulfo-NHS-LC-Biotin (Thermo Fisher Scientific, catalog number A39257), according to the manufacturer's instructions, with a biotin-to-protein molar ratio of 1:12. The detection reagent contained a secondary antibody [Alexa Fluor 647 goat anti-human IgG (Thermo Fisher Scientific, reference number A21445)] diluted in Rxxip F (Gyros Protein Technologies, reference number P0004825; 1:500 dilution of the 2 mg/ml stock to yield a final concentration of 4 μ g/ml). Buffer phosphate-buffered saline, 0.01% Tween 20 (PBS-T) and Gyros Wash buffer (Gyros Protein Technologies, reference number P0020087) were prepared according to the manufacturer's instructions. Plasma or serum samples were then diluted 1:100 in PBS-T and tested with the Bioaffy 1000 CD (Gyros Protein Technologies, reference number P0004253) and the Gyrolab xPand (Gyros Protein Technologies, reference number P0020520).

Statistical Analysis

GraphPad Prism and R were used for statistical analysis. We applied multinomial logistic regression models between patient groups using IFN response phenotypes and accounting for impacts of age and sex (known factors associated with COVID-19 severity) using the “nnet” (version 7.3) R package . For comparison of patient subgroups with smaller sample sizes, non-parametric Kruskal-Wallis tests, followed by Dunn's post-test for multiple group comparisons were performed. Significance cut offs are denoted as follows *P < 0.05; **P < 0.01; ***P < 0.001. Correlations between the different assays were calculated using Spearman test. UMAP plots were performed with “M3C” R package (v1.10.0). Gene set enrichment analysis (GSEA) was performed as previously described² using a pathway data set built from the Nanostring Host response panel annotation file. Heatmaps were produced with Qlucore (version 3.5). Dot plots and correlation graphs were produced with GraphPad Prism (version 9).

Results

Decreased blood IFN α protein, ISGs and activity in severe and critical COVID-19 patients

We previously reported lower plasma IFN α 2 levels in COVID-19 patients with severe and critical disease, when assessed 8-12 days post-symptom onset ². A multinomial logistic

regression model integrating age and sex showed significantly higher levels of plasma IFN α 2 in moderate (P=0.005) and severe (P=0.03) disease compared to uninfected controls, but no increase in the critical group (P=0.33) (Fig. 1a). Using the moderate group as the reference, significantly (P=0.02) lower levels were present in the critical group (Fig. 1a). To test if this was also observed for all 13 IFN α subtypes, we applied the multi IFN α subtypes digital ELISA (measured as the equivalent of IFN α 17) and observed a similar pattern, with significantly higher levels of all IFN α subtypes in moderate (P=0.002) and severe (P=0.005), and also a significant increase in critical patients (P=0.01), as compared to non-infected healthy controls. Using the moderate group as the reference, significantly (P=0.005) lower levels were present in the critical group (Fig. 1a). Due to conflicting reports on IFN α levels in other studies using non-digital assays, we assessed IFN α 2 in the same samples using a commercial Luminex assay. Strikingly, results from this assay showed no differences between controls and moderate, severe, and critical COVID-19 patients (Fig. 1c). To test which protein assay best reflected *in vivo* activity, we correlated measurements from each assay with an ISG score (6 gene score, previously validated²) (Fig. 1d, e, f), and with IFN activity measured by a functional cytopathic assay previously described² (Fig. 1g, h, i). IFN α 2 and multi IFN α subtype proteins measured by digital ELISA showed good positive correlations with both ISG score (Rs=0.69, Rs=0.82) (Fig 1d, e) and functional activity (Rs=0.51, Rs=0.57) (Fig 1g, i), in contrast with the Luminex values which did not correlate with either ISG score (Rs=0.07) (Fig 1f) or functional activity (Rs=0.12) (Fig. 1i). The two digital ELISA measures strongly correlated with each other (Fig. S1a), but neither correlated with the Luminex values (Fig. S1b, c). These collective results highlight the importance of using sensitive and qualified assays for studying IFN-I from patient samples. In contrast to IFN α , we detected no IFN β in these plasma samples using a Simoa assay with a limit of detection of 0.6pg/ml (Fig. S1d).

To validate our results in an independent cohort, and also assess potential differences with non-alpha SARS-CoV-2 viral variants, we applied the three IFN α assays to another cohort of COVID-19 patients recruited during a different wave of infection when the delta variant was prominent (Dec 2020-April 2021). The overall pattern of results was similar with the lowest protein levels observed in critical patients using the digital ELISAs (Fig 1j, k), and no differences between patient groups using Luminex (Fig. 1l). Multimodal logistic regression models integrating age and sex, using the moderate group as a reference, showed significantly lower IFN α 2 (P=0.04) and multi IFN α subtype (P=0.01) proteins in the critical patient group. Interestingly much greater heterogeneity (5 logs of variability compared to 3) was observed in the IFN α plasma levels in this replication cohort compared to the first cohort (Fig 1a, b, c) likely

reflecting a more diverse and older patient cohort (median ages; 55 cohort 1 and 66 years cohort 2, $P < 0.001$) (Table S3). As in the first cohort, the two digital ELISA measures strongly correlated with each other (Fig. S1e), but neither correlated with the Luminex values (Fig. S1f, g). These results highlight the challenges in comparing cytokine responses across patient cohorts with different underlying characteristics and the importance of considering such clinical variables in the interpretation of immune data during active infection.

Given the high variability observed in IFN-I plasma levels, as well as the challenges of obtaining samples from early in infection, we tested whether we could observe significant differences in IFN-I protein levels between COVID-19 patients that were either non-hospitalized or hospitalized based on their requirement for oxygen supplementation. For this analysis, patients were recruited at St James's Hospital (SJH) in Dublin, Ireland as described in the methods. Multimodal regression models incorporating age and sex, and using healthy controls as the baseline showed a significant ($P=0.008$) increase in IFN α 2 (Fig 2a) levels in non-hospitalized, but not hospitalized patients ($P=0.24$). In contrast, results with the multi IFN α subtype assay showed a significant increase in all subtypes in both non-hospitalized ($P=0.04$) and hospitalized patients ($P=0.03$) (Fig 2b). Confirming these potential IFN α subtype differences a direct comparison between the two COVID-19 patients groups showed a significant difference ($P=0.004$) in IFN α 2 levels only (Fig 2a, b). In agreement with the previous results, IFN β levels were undetectable in the majority of patients, with no differences between the groups and controls (Fig. S2a). An ISG score (Z score on interferon response genes (IRGs) measured by nanostring, described in methods) in paired whole blood samples correlated positively and significantly with both Simoa IFN α measures (IFN α 2: $R_s=0.36$ $p=0.005$ Fig2b, and multi IFN α subtype: $R_s=0.42$, $p=0.002$ Fig 2c); but not IFN β (Fig. S2d).

Given the observed differences in IFN α 2, but not all IFN α subtypes, at the plasma protein level, we further explored potential differences in IFN α subtype expression using Nanostring gene expression data on whole blood. This showed low transcriptional levels of all measured *IFNA* subtypes as expected (Fig. S2b). Despite these low baseline levels, among the 7 *IFNA* subtypes examined we did observe some subtype differences, with notably higher levels of *IFNA6* in both COVID-19 patient groups and *IFNA1/13* and *IFNA5* only in the hospitalized group (Fig. S2b). *IFNA2* was notably no different between all three groups (Fig. S2e).

Given the previously reported importance of autoantibodies as a risk factor for severe COVID-19⁴, and their potential to interfere with IFN α protein measurements²⁴, we quantified anti-IFN α (Fig 2c) and anti-IFN ω (Fig 2d) autoantibodies by Gyros assay. Among the 126 patients tested, 4 were identified as anti-IFN α autoantibody positive (>95 considered positive)

and all were male patients (aged 31, 53, 81, and 85 years old) in the hospitalized group with mixed severities at time of sampling (2 moderate, 1 severe, 1 critical) (Fig 2c). Interestingly, of these 4 patients, multi IFN α subtypes results were extremely low (Fig. S2g), although 2 had elevated levels with the IFN α 2 assay (Fig. S2f). We previously described how recognition of IFN α 2 in this specific assay is not always blocked by autoantibodies from all autoantibody-positive individuals²⁴, likely due to recognition of a non-functional epitope in contrast with the multi IFN α subtypes assay. However, the majority of patients were negative for anti-IFN autoantibodies suggesting that this was not the driver of severe disease in these patients.

We next assessed whether IFN α levels changed with time post-symptoms in either patient group. IFN α 2 (Fig 2e) and multi IFN α subtypes (Fig 2f) levels mostly declined with time post-symptoms in both patient groups (non-hospitalized; slope= 3.4, -3.2, and hospitalized R= -0.33, -0.41) with no significant differences in the decline ($p=0.47$, $p=0.68$ for IFN α 2 and multi IFN α subtypes respectively) between the two patient groups (Fig. 2e, f). IFN β levels although lower to begin with, also followed the same decline with time post-symptoms with no significant difference ($p=0.12$) between the two patient groups (Fig. S2h).

Induction of type I interferon is compromised in hospitalized patients

Our results thus far demonstrating lower IFN α plasma levels in severe disease, yet similar kinetics across COVID-19 disease states, suggests that induction of IFN-I in the absence of autoantibodies is critical to understand defective anti-viral immunity in severe COVID-19. To investigate the functional IFN capacity of COVID-19 patients, whole blood from a sub cohort of patients was stimulated with immune agonists relevant for anti-viral immune pathway activation, namely Poly:IC (a synthetic analog of double-stranded RNA and reported TLR3/MDA5 agonist), R848 (a small molecular weight imidazoquinoline compound and TLR7/8 agonist), as well as LPS (Lipopolysaccharide (LPS) synthesized by *E. coli* and a TLR4 agonist), and a Null condition as positive and negative controls, respectively. At 22hrs, IFN α 2 was weakly induced by Poly:IC stimulation, but strongly induced by R848 (Fig. 3a). Measurement of all IFN α subtypes revealed a broader response with the highest levels in moderate patients (Fig. 3b). Multinomial logistic regression models integrating age and sex, and using the healthy group as the reference, showed significantly higher ($P=0.01$) multi IFN α subtype levels in non-hospitalized moderate patients after Poly:IC ($P=0.01$) and LPS ($P=0.002$) stimulation, but not in more severe patients (Fig 3b). More striking was the IFN β response which was significantly reduced ($P<0.001$) after Poly:IC stimulation in both COVID-19 groups

compared to controls, but also significantly reduced after R848 ($P=0.005$) and LPS ($P=0.04$) stimulation in only the hospitalized groups (Fig. 3c).

To assess whether differences in receptor expression could explain these cytokine differences, we examined the relevant TLR gene expression data from whole blood. Expression of *TLR7* was similar in all groups, while expression of *TLR3* was significantly lower, and of *TLR4* and *TLR8* was significantly higher, in hospitalized patients. Expression of *IFIH1* was higher in both patient groups, although the effects were modest and the differences are unlikely to explain the differences in cytokine responses (Fig. 3d). To examine whether these immune differences were restricted to IFN-I responses, we measured an additional 42 cytokines in the whole blood stimulations by Luminex (Fig. S3). This revealed 8 additional cytokines with significant differences in hospitalized patients, mostly after TLR3 stimulation. However, half of these differential cytokines (CXCL10, IL-12p70, CCL4, and IL-10), which were all lower in hospitalized patients after Poly:IC stimulation, are downstream of IFN-I responses. This further supports the finding of defective IFN-I responses in unfavorable COVID-19 states.

To confirm these observations in an independent cohort of COVID-19 patients with more severe disease, we sampled additional hospitalized patients from two Parisian clinical centers. Given previous studies indicating age and sex as strong risk factors, we also recruited severe and critical patients with similar ages (medians; 63 and 76 years old respectively, $P=0.05$) and sex distribution (40% and 26% female, Fisher test 0.7) (Table S3). We also tested lower agonist concentrations, to assess more subtle induction of IFN-I responses and avoid potential over-stimulation, to which acutely infected patients may be more sensitive. In this independent cohort, we again observed a strongly reduced IFN α 2 (Fig. 3e-g) and IFN β (Fig. 3h-j) secreted response to Poly:IC, LPS and R848 stimulation in critical COVID-19 patients in comparison to healthy controls. Severe COVID-19 patients showed an intermediate response. We also included a live viral stimulus (influenza H1N1 PR8 strain), to which the IFN-I (IFN α 2 and IFN β) response was also significantly reduced as the disease severity increased (Fig. 3k, l). Collectively these results show a broadly perturbed type I interferon response to diverse immune stimulation that increases with disease severity.

Compromised interferon responses at the cellular level with increasing COVID-19 severity

Previous studies have reported multiple cellular and intracellular perturbations in patients with moderate as well as severe COVID-19. To test whether changes in either cell numbers, or

interferon regulatory transcription factors (IRFs), could explain the severely reduced IFN responses to pattern recognition receptor (PRR) stimulation, we performed multi-parameter intra-cellular flow cytometry on the blood of hospitalized COVID-19 patients (Table S5 Fig S4a). In line with previous findings, we observed a significant increase in circulating granulocytes and monocytes, in parallel to a significant decline in T cells and pDCs, in critically infected patients confirming that our cohort exhibited the typical immunological dysregulation associated with increasing severity of COVID-19 (Fig. 4a). To assess IFN-I signaling pathways we measured intracellular phosphorylated IRF3 and IRF7, and intracellular IFN α 2 after R848 stimulation (Fig. S4b, c, d). Analysis of the percentage of positive cells and mean fluorescent intensity (MFI) showed that pIRF7 significantly increased in different monocyte subsets and pDCs of healthy donors after R848 stimulation (Fig. S4b). Changes in pIRF3 and intracellular IFN α 2 were more modest, but were also detectable in monocytes and pDCs after R848 stimulation (Fig. S4c, d).

As our data showed that both pDC and monocyte cell subsets are major regulators of the type I IFN response in human blood in response to R848, we therefore focused on these cell types in COVID-19 patients. We observed a significant increase in pIRF7 in monocytes from severe and critical groups (Fig 4b). However, this was not matched by an increase in intracellular IFN α 2, perhaps due to the lack of induction of pIRF3 (Fig 4c), or the elevated intracellular IFN α 2 at the baseline in the absence of stimulation (Fig 4d) in both severe and critical patients. In pDCs of COVID-19 patients, pIRF7 was also significantly increased after R848 stimulation (Fig 4e), but in contrast to the monocytes this was matched by an increase in intracellular IFN α in severe, but not in critical patients (Fig 4g). Additional correlation analysis between cytometry measured intracellular IFN α , and digital ELISA measured plasma IFN α , showed in the absence of stimulation an association between monocytes and plasma IFN α levels (Fig. 4d). Following R848 stimulation, both pDCs and monocytes showed an association with secreted IFN α (Fig 4h), although the percentage of IFN α ⁺ cells was lower in critical patients compared to severe and healthy controls (Fig. 4i). Collectively these results indicate a perturbation of IFN signaling networks in elevated numbers of circulating monocytes in all hospitalized COVID-19 patients. pDCs demonstrate a quantitative decrease in disease states but retain functional responsiveness in severe disease. This pDC functional response is lost in critical disease.

Induced gene expression changes identify consistently perturbed myeloid associated pathways

To further explore potential reasons behind the perturbed IFN-I responses in hospitalized patients we examined gene expression differences after immune stimulation between hospitalized and non-hospitalized patients in the St. James cohort. To do this, we applied UMAP (Uniform Manifold Approximation and Projection for Dimension Reduction) to 800 immunology and host response related genes measured by Nanostring in each condition (Null, PolyI:C, LPS, and R848) (Fig. 5a). This revealed clustering of the hospitalized patients and healthy controls, with the non-hospitalized patients spread between the two groups in all conditions including the unstimulated control. This suggests that induced immune responses are already perturbed at baseline in hospitalized COVID-19 patients. This highlights their already dysregulated state and is in line with the altered circulating IFN-I levels we observed. PolyI:C revealed the most distinct clusters, with hospitalized patients separating from controls along dimensions 1 and 2 (Fig. 5a).

To examine differences at a biological pathway level, we applied gene set enrichment analysis (GSEA) to each stimulation condition specifically comparing healthy controls *versus* non-hospitalized (Fig. 5b), controls *versus* hospitalized (Fig. 5c), and non-hospitalized *versus* hospitalized (Fig. 5d). The most significant pathway differences were observed in the healthy *versus* mild non-hospitalized comparison. As expected from our previous findings and in line with circulating IFN-I measurements, the null state of mild patients showed upregulation of type I and II IFN pathways, and these pathways were preferentially upregulated after R848 stimulation in controls (Fig. 5b, in black). Non-hospitalized COVID-19 patients also showed upregulated IL-17 responses, prostaglandin, and TGFB and HIF signaling to Poly:IC, LPS, and R848 stimulation (Fig. 5b, in green). Gene pathway alterations in hospitalized COVID-19 patients revealed consistently perturbed myeloid activation in unstimulated conditions and after Poly:IC stimulation, when compared with controls (Fig. 5c) and non-hospitalized patients (Fig. 5d). Additional pathways upregulated in hospitalized patients included coagulation, complement system, and TLR and MAPK signaling (Fig. 5c & d, in orange).

IFN-I stimulation drives non-canonical inflammatory signaling in hospitalized patients only

Finally, after identifying perturbations in baseline and induced IFN responses, we wanted to assess the direct signaling response to IFN-I in COVID-19 patients. For this, we performed the same standardized whole blood *ex vivo* stimulation with recombinant IFN α 2 and measured gene expression by Nanostring as previously described. Application of an ISG z score showed that non-hospitalized and hospitalized patients were unable to induce classical ISG response

following direct IFN α stimulation, as was also the case with Poly:IC and R848 stimulations (Fig. 6a). This was likely explained by the already elevated ISG score in the Null condition of these patients. To apply a less biased analysis, we defined all genes that were significantly induced by IFN α stimulation across the entire cohort (q value < 0.05, Log 1.3-fold change compared to Null condition). Application of these 200 genes (Table S6) to a heat map clustered by gene response and grouped by clinical category revealed interesting differences (Fig. 6b). 50% of the genes were only induced in controls, and pathway analysis showed that these genes were classically involved in IFN-I and anti-viral responses (Fig. 6c), as exemplified by *MXI* (Fig. 6d). An additional group of genes were upregulated in both controls and non-hospitalized patients, that included *TLR3*, *TLR7*, *CXCL10*, *CXCL11*, and HLA molecules (Fig. 6b, e). Most interestingly, a third cluster of genes was differentially expressed in hospitalized patients only, with pathway analysis showing this to consist largely of an inflammatory response (Fig. 6f, g). Many of these genes were downregulated after IFN α stimulation in controls and mild patients, but not in hospitalized patients, as exemplified by *IL1RI* (Fig. 6g). One hospitalized patient was identified to be positive for anti-IFN autoantibody (indicated by an * on the heat map, Fig. 6b). Strikingly this individual patient clearly lacked a classical ISG response to *ex vivo* IFN α stimulation, but their response to this non-canonical inflammatory activity was not affected.

Discussion

Type I interferons mediate the major innate anti-viral immune activities through activation of hundreds of genes. However, due to complex regulation of their diverse functions, as well as their inhibition by many viruses, the precise role and impact of IFN-I in disease pathogenesis is not always evident. In COVID-19, the protective importance of IFN-I was evidenced by identification of negative impacts on early IFN-I as strong risk factors for severe disease. These include neutralizing autoantibodies against IFN α , IFN ω , and IFN β ^{4,5}, as well as inborn errors of immunity in IFN-mediated pathways including *TLR3*³ and *TLR7*⁷. Additional genetic evidence in support of a protective role for IFN-I in COVID-19 has also come from genome-wide association studies. These identified genome-wide associations between severe COVID-19 and gene clusters in *IFNAR2* (subunit of IFN receptor), near the gene encoding tyrosine kinase 2 (*TYK2*) (associates with plasma domain of *IFNAR*), and in a gene cluster encoding antiviral restriction enzyme activators (*OAS1*, *OAS2*, *OAS3*) (induced by IFN-I)²⁹. Highlighting the complex role of ISGs in viral responses, and the need for careful interpretation, mendelian randomization showed a link between life-threatening disease and low expression of *IFNAR2*, but high expression of *TYK2*²⁹. However, although these associations had genome

wide significance, the effect sizes were relatively modest (OR 1.3-1.6). Despite these collective studies highlighting how critical IFN-I immunity is in dictating COVID-19 outcome, cumulatively, they cannot account for the majority of the defective IFN-I responses observed in severe COVID-19. Furthermore elevated IFN β has been recently implicated in long COVID-19, emphasizing the need to better understand the regulation of IFN-I during infection with SARS-CoV-2.

Our study adds further knowledge to why IFN-I responses are defective in severe COVID-19 through two major findings: first, we show that a combination of decreased circulating pDC numbers and dysregulated monocytes in critical disease is a major cause of ineffective IFN α secretion and second, IFN-I stimulation of leukocytes from severe COVID-19 patients promotes an inflammatory response that was not observed in moderate patients.

Undoubtedly some of the early confusion around the role of systemic IFN in COVID was due to the different assays used to measure the cytokine directly. A meta-analysis comparing 15 studies that used either ELISA, single molecular array (Simoa) digital ELISA, Luminex, electrochemiluminescent, flow cytometry bead-based immunoassay and microfluid immunoassay fluorescence detection techniques, showed no significant differences in plasma levels between different disease severities²². However, our results presented here highlight the importance of using sufficiently sensitive assays for measuring IFN α proteins, as physiological concentrations are often below pg/mL levels^{23,24}. When such assays are applied to COVID-19 patient samples, more consistent results were observed, with severe patients overall showing lower levels of circulating IFN α ^{2,14,30,31,32,33}. Nevertheless, our results in more heterogeneous patient populations with co-morbidities and older ages revealed a larger range of IFN α levels, highlighting the challenges of comparing across studies and for translating to possible clinical applications. The presence of 13 IFN α subtypes can also lead to confusion, with many assays used not reporting the subtype measured. A recent *in vitro* study reported different anti-SARS-CoV-2 functional activity between the diverse IFN α subtypes, and here we observed differences in IFN α 2 protein plasma levels, but not total subtype levels, between moderate and severe disease. New experimental tools will be needed to fully understand the different roles of all IFN α subtypes in COVID-19 patients, which given their previously reported evolutionary selection³⁴, may be relevant for other viral infections.

Poor results in randomized placebo controlled treatment studies have further divided opinion on the importance of IFN-I in COVID-19^{8,9}. No clinical benefit was observed in these studies where either IFN α or IFN β were given alone, or in combination with antivirals. However, a major caveat of these studies is the late initiation of treatment when patients were

unlikely to benefit from further antiviral signaling. Moreover, at this stage of infection, IFN-I may even suppress adaptive immunity, further compromising any apparent clinical benefit. This is supported by results from our study where COVID-19 patients with elevated ISG expression did not respond to *ex vivo* IFN stimulation, and hospitalized patients in particular showed an inflammatory gene expression pattern that was not down regulated by IFN-I. Direct testing of this hypothesis may be provided by clinical studies testing early intervention prior to appearance of symptoms³⁵ or targeted to patients with known risk factors³⁶, or retrospective testing of pre-treatment IFN-I levels. Reflecting multiple perturbations in the IFN-I response with increasing COVID-19 severity was our striking observation that severe patients failed to secrete IFN-I proteins after stimulation with diverse viral agonists. This supports previous results showing a reduced ability of pDCs and monocytes from COVID-19 patients to respond to TLR stimulation³³. IFN β secretion was even more strikingly perturbed than IFN α , which was surprising given its low levels in patient plasma. However, the relatively low number of studies implicating this IFN subtype in COVID-19 are indicative of the challenges in accurately detecting and quantifying this interferon in the blood, and may reflect its greater importance in the infected tissues.

Why such broad IFN protein responses are blunted in COVID-19 patients remains unexplained, beyond the impact of neutralizing autoantibodies^{4,5} and inborn errors of IFN-I immunity^{3,7}. It is possible that lower concentrations of autoantibodies, below detection limits of current assays, may be clinically relevant in certain patients but our intra-cellular cytokine data suggests this is not the case. While the SARS-CoV-2 virus has been shown to interfere with many aspects of host immunity³⁷, we studied blood immune cell responses where presence of the virus was undetectable by droplet digital PCR. Therefore, it is unlikely that this phenotype could be directly attributed to viral interference. While pDCs numbers were reduced with increasing severity, they still remained capable of producing IFN α as measured intracellularly, in line with previous *in vitro* studies³⁸. In contrast, monocytes which were increased in the circulation with severity appeared to express IFN α intracellularly in the steady state, but did not increase production or secretion after TLR stimulation. Further functional analysis of intracellular pathways in isolated cells from severe COVID-19 patients will be required to fully understand this phenotype, which may provide targets for new treatment strategies.

Acknowledgments

This study was supported by the “URGENCE COVID-19” fundraising campaign the Institut Pasteur (CoVarImm and Steroid Response), from the Agence Nationale de la Recherche (ANR-flash COVID-19), by the Laboratoire d’Excellence ‘Milieu Intérieur’ (grant no. ANR-10-LABX-69-01), the Fonds IMMUNOV for Innovation in Immunopathology, and Science Foundation Ireland. We thank the STTAR-Bioresource of TCD-SJH-TUH COVID-19 bioresource which supported collection of patient samples. NS is a recipient of the Pasteur-Roux-Cantarini Fellowship. COF, NC and CNC are part-funded by a Science Foundation Ireland (SFI) grant, Grant Code 20/SPP/3685. LT is supported by the Irish Clinical Academic Training (ICAT) Programme, supported by the Wellcome Trust and the Health Research Board (Grant Number 203930/B/16/Z), the Health Service Executive, National Doctors Training and Planning and the Health and Social Care, Research and Development Division, Northern Ireland. N.B. is funded under the Science Foundation Ireland Phase 2 COVID-19 Rapid Response Call (20/COV/8487) and the Health Research Board COVID-19 Rapid Response Call (COV19e2020e053). The Laboratory of Human Genetics of Infectious Diseases is supported by the Howard Hughes Medical Institute, the Rockefeller University, the St. Giles Foundation, the National Institutes of Health (NIH) (R01AI088364 and R01AI163029), the National Center for Advancing Translational Sciences (NCATS), NIH Clinical and Translational Science Award (CTSA) program (UL1 TR001866), a Fast Grant from Emergent Ventures, Mercatus Center at George Mason University, the Fisher Center for Alzheimer’s Research Foundation, the Meyer Foundation, the JPB Foundation, the French National Research Agency (ANR) under the “Investments for the Future” program (ANR-10-IAHU-01), the Integrative Biology of Emerging Infectious Diseases Laboratory of Excellence (ANR-10-LABX-62-IBEID), the French Foundation for Medical Research (FRM) (EQU201903007798), , the ANRS-COV05, ANR GENVIR (ANR-20-CE93-003), ANR AABIFNCOV (ANR-20-CO11-0001) and ANR GenMISC (ANR-21-COVR-0039) projects, the European Union’s Horizon 2020 research and innovation programme under grant agreement No 824110 (EASI-genomics), the Square Foundation, Grandir - Fonds de solidarité pour l’enfance, the Fondation du Souffle, the SCOR Corporate Foundation for Science, The French Ministry of Higher Education, Research, and Innovation (MESRI-COVID-19), Institut National de la Santé et de la Recherche Médicale (INSERM), REACTing-INSERM and the University of Paris. PB was supported by the MD-PhD program of the Imagine Institute (with the support of the Fondation Bettencourt-Schueller). We thank the UTechS CB of the Center for Translational Research, Institut Pasteur for supporting Luminex and Nanostring analysis. We acknowledge all health-care workers

involved in the diagnosis and treatment of patients in Hopital Cochin, Hopital Bichat, and St James's Hospital Dublin.

References

1. Bastard, P., Zhang, Q., Zhang, S.-Y., Jouanguy, E. & Casanova, J.-L. Type I interferons and SARS-CoV-2: from cells to organisms. *Curr Opin Immunol* **74**, 172–182 (2022).
2. Hadjadj, J. *et al.* Impaired type I interferon activity and inflammatory responses in severe COVID-19 patients. *Science* **369**, 718–724 (2020).
3. Zhang, Q. *et al.* Inborn errors of type I IFN immunity in patients with life-threatening COVID-19. *Science* (2020) doi:10.1126/science.abd4570.
4. Bastard, P. *et al.* Auto-antibodies against type I IFNs in patients with life-threatening COVID-19. *Science* (2020) doi:10.1126/science.abd4585.
5. Bastard, P. *et al.* Autoantibodies neutralizing type I IFNs are present in ~4% of uninfected individuals over 70 years old and account for ~20% of COVID-19 deaths. *Sci Immunol* **6**, eabl4340 (2021).
6. Zhang, Q., Bastard, P., COVID Human Genetic Effort, Cobat, A. & Casanova, J.-L. Human genetic and immunological determinants of critical COVID-19 pneumonia. *Nature* (2022) doi:10.1038/s41586-022-04447-0.
7. Asano, T. *et al.* X-linked recessive TLR7 deficiency in ~1% of men under 60 years old with life-threatening COVID-19. *Science Immunology* **6**, (2021).
8. WHO Solidarity Trial Consortium *et al.* Repurposed Antiviral Drugs for Covid-19 - Interim WHO Solidarity Trial Results. *N Engl J Med* (2020) doi:10.1056/NEJMoa2023184.

9. Kalil, A. C. *et al.* Efficacy of interferon beta-1a plus remdesivir compared with remdesivir alone in hospitalised adults with COVID-19: a double-blind, randomised, placebo-controlled, phase 3 trial. *The Lancet Respiratory Medicine* **0**, (2021).
10. Schultze, J. L. & Aschenbrenner, A. C. COVID-19 and the human innate immune system. *Cell* **184**, 1671–1692 (2021).
11. Lucas, C. *et al.* Longitudinal analyses reveal immunological misfiring in severe COVID-19. *Nature* **584**, 463–469 (2020).
12. Broggi, A. *et al.* Type III interferons disrupt the lung epithelial barrier upon viral recognition. *Science* **369**, 706–712 (2020).
13. Krämer, B. *et al.* Early IFN- α signatures and persistent dysfunction are distinguishing features of NK cells in severe COVID-19. *Immunity* S1074761321003654 (2021) doi:10.1016/j.immuni.2021.09.002.
14. Venet, F. *et al.* Longitudinal assessment of IFN-I activity and immune profile in critically ill COVID-19 patients with acute respiratory distress syndrome. *Critical Care* **25**, 140 (2021).
15. Thwaites, R. S. *et al.* Inflammatory profiles across the spectrum of disease reveal a distinct role for GM-CSF in severe COVID-19. *Science Immunology* **6**, (2021).
16. Lee, J. S. *et al.* Immunophenotyping of COVID-19 and influenza highlights the role of type I interferons in development of severe COVID-19. *Sci Immunol* **5**, (2020).
17. Blanco-Melo, D. *et al.* Imbalanced Host Response to SARS-CoV-2 Drives Development of COVID-19. *Cell* **181**, 1036-1045.e9 (2020).
18. Galbraith, M. D. *et al.* *Specialized interferon ligand action in COVID19.* 2021.07.29.21261325 <https://www.medrxiv.org/content/10.1101/2021.07.29.21261325v1> (2021) doi:10.1101/2021.07.29.21261325.

19. Schuhenn, J. *et al.* Differential interferon- α subtype induced immune signatures are associated with suppression of SARS-CoV-2 infection. *PNAS* **119**, (2022).
20. Sposito, B. *et al.* Severity of SARS-CoV-2 infection as a function of the interferon landscape across the respiratory tract of COVID-19 patients. 2021.03.30.437173 <https://www.biorxiv.org/content/10.1101/2021.03.30.437173v1> (2021) doi:10.1101/2021.03.30.437173.
21. Smith, N. *et al.* Distinct systemic and mucosal immune responses during acute SARS-CoV-2 infection. *Nat Immunol* **22**, 1428–1439 (2021).
22. da Silva, R. P., Gonçalves, J. I. B., Zanin, R. F., Schuch, F. B. & de Souza, A. P. D. Circulating Type I Interferon Levels and COVID-19 Severity: A Systematic Review and Meta-Analysis. *Frontiers in Immunology* **12**, 1717 (2021).
23. Rodero, M. P. *et al.* Detection of interferon alpha protein reveals differential levels and cellular sources in disease. *J. Exp. Med.* **214**, 1547–1555 (2017).
24. Bondet, V. *et al.* Differential levels of IFN α subtypes in autoimmunity and viral infection. *Cytokine* 155533 (2021) doi:10.1016/j.cyto.2021.155533.
25. Duffy, D. *et al.* Standardized whole blood stimulation improves immunomonitoring of induced immune responses in multi-center study. *Clin. Immunol.* **183**, 325–335 (2017).
26. Darnell, M. E. R. & Taylor, D. R. Evaluation of inactivation methods for severe acute respiratory syndrome coronavirus in noncellular blood products. *Transfusion* **46**, 1770–1777 (2006).
27. Duffy, D. *et al.* Functional analysis via standardized whole-blood stimulation systems defines the boundaries of a healthy immune response to complex stimuli. *Immunity* **40**, 436–450 (2014).

28. Piasecka, B. *et al.* Distinctive roles of age, sex, and genetics in shaping transcriptional variation of human immune responses to microbial challenges. *Proc. Natl. Acad. Sci. U.S.A.* **115**, E488–E497 (2018).
29. Pairo-Castineira, E. *et al.* Genetic mechanisms of critical illness in Covid-19. *Nature* 1–1 (2020) doi:10.1038/s41586-020-03065-y.
30. Flament, H. *et al.* Outcome of SARS-CoV-2 infection is linked to MAIT cell activation and cytotoxicity. *Nat Immunol* **22**, 322–335 (2021).
31. Trouillet-Assant, S. *et al.* Type I IFN immunoprofiling in COVID-19 patients. *J Allergy Clin Immunol* **146**, 206-208.e2 (2020).
32. Dorgham, K. *et al.* Distinct cytokine profiles associated with COVID-19 severity and mortality. *Journal of Allergy and Clinical Immunology* S0091674921006515 (2021) doi:10.1016/j.jaci.2021.03.047.
33. Arunachalam, P. S. *et al.* Systems biological assessment of immunity to mild versus severe COVID-19 infection in humans. *Science* **369**, 1210–1220 (2020).
34. Manry, J. *et al.* Evolutionary genetic dissection of human interferons. *J. Exp. Med.* **208**, 2747–2759 (2011).
35. Iturriaga, C. *et al.* A cluster randomized trial of interferon β -1a for the reduction of transmission of SARS-Cov-2: protocol for the Containing Coronavirus Disease 19 trial (ConCorD-19). *BMC Infect Dis* **21**, 814 (2021).
36. Bastard, P. *et al.* Interferon- β Therapy in a Patient with Incontinentia Pigmenti and Autoantibodies against Type I IFNs Infected with SARS-CoV-2. *J Clin Immunol* 1–3 (2021) doi:10.1007/s10875-021-01023-5.
37. Jouvenet, N., Goujon, C. & Banerjee, A. Clash of the titans: interferons and SARS-CoV-2. *Trends Immunol* **42**, 1069–1072 (2021).

38. Onodi, F. *et al.* SARS-CoV-2 induces human plasmacytoid pre-dendritic cell diversification via UNC93B and IRAK4. 40.
39. Cingöz, O. & Goff, S. P. Cyclin-dependent kinase activity is required for type I interferon production. *Proc Natl Acad Sci U S A* **115**, E2950–E2959 (2018).
40. Bouhaddou, M. *et al.* The Global Phosphorylation Landscape of SARS-CoV-2 Infection. *Cell* **182**, 685-712.e19 (2020).
41. Singh, M. *et al.* A virus-encoded microRNA contributes to evade innate immune response during SARS-CoV-2 infection. 2021.09.09.459577
<https://www.biorxiv.org/content/10.1101/2021.09.09.459577v1> (2021)
 doi:10.1101/2021.09.09.459577.

Figure Legends

Fig 1. Plasma IFN α is consistently reduced with increasing severity of Covid-19. (a) IFN α 2 (left) and (b) multi IFN α subtypes (= equivalent IFN α 17) were measured by Simoa digital ELISA or (c) Luminex in healthy controls (n = 11 donors) and in patients with mild-to-moderate (n = 14), severe (n = 13) and critical (n = 24) disease from the first Hopital Cochin cohort. Interferon-stimulated gene (ISG) score (6 gene score) correlated with IFN α levels measured by (d) Simoa IFN α 2 (e) Simoa multi IFN α subtypes or (f) Luminex; n = 62. IFN activity (IU/mL) correlated with IFN α levels measured by (g) Simoa IFN α 2 (h) Simoa multi IFN α subtypes or (i) Luminex IFN α 2; n = 62. (j) IFN α 2, (k) multi IFN α subtypes (= equivalent IFN α 17) were measured by Simoa digital Elisa or (l) IFN α 2 by Luminex in patients with mild-to-moderate (n = 35), severe (n = 32) and critical (n = 22) disease from the second Hopital Cochin cohort. Lines indicate median values. P values were determined by multimodal regression models incorporating age and sex., Rs represents the Spearman coefficient. Healthy control = black, moderate COVID-19 patients = blue, severe COVID-19 patients = purple and critical COVID-19 patients = red. *P < 0.05; **P < 0.01; ***P < 0.001.

Fig 2. Plasma IFN α is consistently reduced in hospitalized patients independent of neutralizing auto-antibodies. (a) IFN α 2 and (b) multi IFN α subtypes (= equivalent IFN α 17) measured by digital ELISA Simoa in healthy controls (n = 12 donors), non-hospitalized (n = 46), or hospitalized (n = 80) COVID-19 patients of the St James Hospital cohort. (c) Anti-IFN α and (d) anti-IFN ω auto-antibodies in plasma of these healthy controls and COVID-19 patients. (e) IFN α 2 and (f) multi IFN α subtypes cytokine levels as a function of the number of days post symptoms, with regression lines per COVID-19 patient groups shown. P values were determined by a multimodal regression models incorporating age and sex,. Rs represents the Spearman coefficient. Lines indicate the median values. Healthy control = black, non-hospitalized COVID-19 patients = green and hospitalized COVID-19 patients = orange. *P < 0.05; **P < 0.01.

Fig 3. Induction of IFN-I response is perturbed in hospitalized patients. (a) IFN α 2, (b) pan-IFN α and (c) IFN β were measured by digital ELISA in healthy controls(n=19), non-hospitalized (n=27) and hospitalized (n=17) COVID-19 patients after 22h of whole blood stimulation with Poly:IC, LPS and R848. (d) mRNA of TLR3/4/7/8 and IFIH1 whole blood gene expression in healthy controls, non-hospitalized and hospitalized COVID-19 patients. IFN α 2 (e, f, g, k) and INF β (h, i, j, l) responses in healthy donors (n=24), severe (n=11) and critical (n=20) COVID-19 patients after variable dose stimulation with Poly:IC (e, h), LPS (f, i), R848 (g, j) and influenza virus (k, l). Black lines represent the medians. P values were determined either by multimodal regression models incorporating age and sex, or by Kruskal–Wallis test followed by Dunn’s post hoc test for multiple comparisons. Healthy controls = black, non-hospitalized COVID-19 patients = green and hospitalized COVID-19 patients = orange, severe = purple and critical patients = red. *P < 0.05; **P < 0.01; ***P < 0.001; ****P < 0.0001.

Fig 4. Perturbed intracellular IFN-I responses in COVID-19 patients. (a) Counts of granulocytes, T cells, classical monocytes, and pDCs in the blood of healthy controls (n=29), severe (n=11) and critical (n=20) COVID-19 patients. Percentages of (b, e) phosphorylated IRF7, (c, f) phosphorylated IRF3, or (d, g) intracellular IFN α positive monocytes (b, c, d) and pDCs (e, f, g) in the blood of healthy controls, severe and critical COVID-19 patients in the absence of stimulation of after overnight stimulation with R848. Correlation of intracellular IFN α 2 measured by flow cytometry with plasma IFN α 2 levels measured by Simoa in (h)

monocytes without stimulation or in (i) pDCs after R848 stimulation. P values were determined by Kruskal–Wallis test followed by Dunn’s post hoc test for multiple comparisons. *P < 0.05; **P < 0.01; ***P < 0.001; ****P < 0.0001.

Fig 5. Induced gene expression differences in mild and hospitalized Covid-19 patients. (a) UMAP plots of Nanostring gene expression in the Null control, and after whole blood stimulation with Poly:IC, LPS, and R848. Gene expression pathways enriched in healthy donors (black, n=19), mild non-hospitalized COVID-19 patients (green, n=27), or hospitalized COVID-19 (orange, n=17) patients after comparisons between (b) healthy and mild, (c) healthy and hospitalized, (d) mild and hospitalized, after whole blood stimulation with Poly:IC, LPS, and R848.

Fig 6. Downstream signaling response to IFN α is perturbed in hospitalized patients.

(a) Type I interferon gene signature (ISG) score calculated from Nanostring data in healthy controls (black, n=19), mild COVID-19 patients (green, n=27), and hospitalized COVID-19 patients (orange, n=17) in the Null control, and after stimulation with IFN α , Poly:IC, and R848. (b) Heat map of all IFN stimulated genes identified from Nanostring data in healthy controls (black), mild COVID-19 patients (green), and hospitalized COVID-19 patients (orange). Pathways identified to be enriched after IFN α stimulation in (c) healthy donors and (f) hospitalized COVID-19 patients. Nanostring gene expression of (d) MX1, (e) TLR3 and TLR7, and (g) IL1R1 in whole blood of healthy controls (black), mild COVID-19 patients (green), and hospitalized COVID-19 patients (orange). Black lines represent the medians. P values were determined with the Kruskal–Wallis test followed by Dunn’s post hoc test for multiple comparisons. *P < 0.05; **P < 0.01; ***P < 0.001; ****P < 0.0001.

Sup Fig 1. Plasma IFN α is consistently reduced with increasing severity in COVID-19 patients. Correlation plots between (a) digital ELISA IFN α 2 and multi IFN α subtypes (= equivalent IFN α 17), (b) digital ELISA IFN α 2 and Luminex IFN α 2, and (c) digital ELISA multi IFN α subtypes levels and Luminex IFN α 2; first Hopital Cochin cohort, n = 62. (d) IFN β was measured by digital ELISA in healthy controls (n = 11 donors) and in patients with mild-to-moderate (n = 14), severe (n = 13) and critical (n = 24) disease. Correlation plots between (e) digital ELISA IFN α 2 and pan-IFN α , (f) digital ELISA IFN α 2 and Luminex IFN α 2 levels, (g) digital ELISA multi IFN α subtypes and Luminex; second Hopital Cochin cohort, n = 89.

Healthy control = black, moderate COVID-19 patients = blue, severe COVID-19 patients = purple and critical COVID-19 patients = red. Rs represents the Spearman coefficient.

Sup Fig 2. Plasma IFN α and neutralizing auto-antibodies in COVID-19 patients.

(a) IFN β was measured by digital ELISA in healthy controls (n = 12 donors) and in COVID-19 patients non-hospitalized (n = 46) or hospitalized (n = 80) of the St James Hospital cohort.. Correlation plots between ISG zScore and (b) digital ELISA IFN α 2 (c) multi IFN α subtypes and (d) IFN β levels measured by Simoa, n = 50. (e) mRNA of IFNA1/13, IFNA14/16, IFNA2, IFNA4/7/10/17/21, IFNA5, IFNA6, and IFNA8 whole blood gene expression in healthy controls, non-hospitalized and hospitalized COVID-19 patients. P values were determined by a Kruskal–Wallis test followed by Dunn’s post hoc test for multiple comparisons Correlation plots between anti-IFN α auto-antibodies and (f) IFN α 2 or (g) multi IFN α subtypes digital ELISA levels. (h) IFN β levels as a function of the number of days post symptoms, with regression lines per COVID-19 patient groups shown. Rs represents the Spearman coefficient. Healthy control = black, non-hospitalized COVID-19 patients = green and hospitalized COVID-19 patients = orange.

Sup Fig 3. Induction of IFN-I response is perturbed in hospitalized patients. GM-CSF (a), IL-12p70 (b), CXCL10 (c), IL-10 (c), Granzyme B (e), CCL4 (f), PDL1 (g) and CXCL2 (h) were measured by Luminex in healthy control non-hospitalized and hospitalized COVID-19 patients after whole blood stimulation with Poly:IC, LPS and R848. Black lines indicate median values.. P values were determined with the Kruskal–Wallis test followed by Dunn’s post hoc test for multiple comparisons. healthy control = black, non-hospitalized COVID-19 patients = green and hospitalized COVID-19 patients = orange. *P < 0.05; **P < 0.01; ***P < 0.001; ****P < 0.0001.

Sup Fig 4. Intra-cellular analysis of pIRF7, pIRF3, and IFN α before and after R848 stimulation. (a) Flow cytometry gating strategy. Percentage of positive cells and MFI of (b) IFR7, (c) IRF3, and intracellular IFN α (d) in immune cell subtypes in whole blood of healthy donors without stimulation or after R848 stimulation.

Table S1. Summary of different COVID-19 patient cohorts and healthy controls included in the different immunological analyses.

Table S2. Patient cohort characteristics of cohort 1.

Table S3. Patient cohort characteristics of cohort 2.

Table S4. Patient cohort characteristics of cohort 3.

Table S5. Patient cohort characteristics of cohort 4.

Table S6. Flow cytometry panel applied to analyze intracellular IFN α and pIRF expression.

Table S7. List of Nanostring genes differentially induced between Null and IFN α stimulations across all donors and patients.

Figures

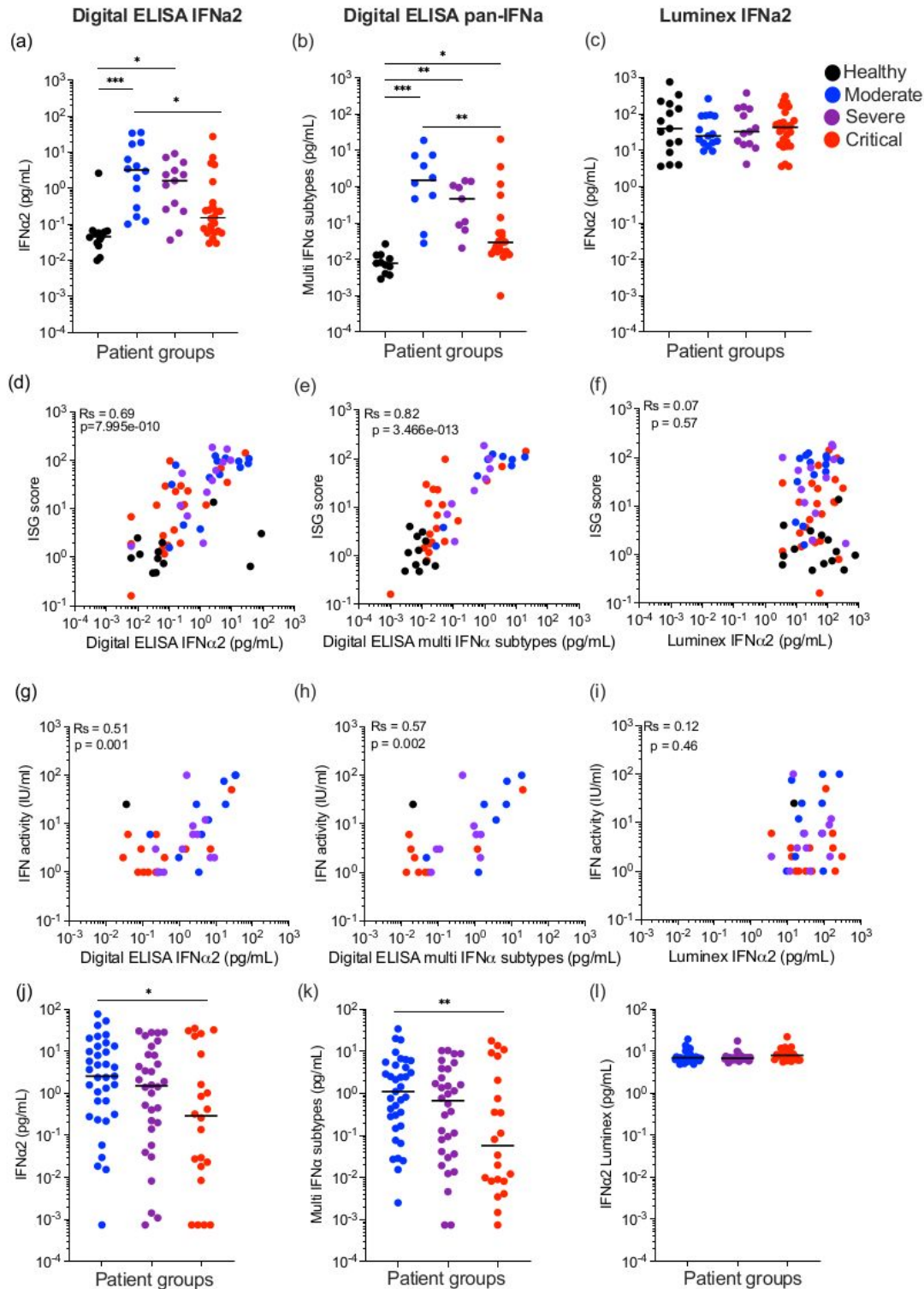


Figure 1

Figure 1

Plasma IFNα is consistently reduced with increasing severity of Covid-19. (a) IFNα2 (left) and (b) multi IFNα subtypes (= equivalent IFNα17) were measured by Simoa digital ELISA or (c) Luminex in healthy controls (n = 11 donors) and in patients with mild-to-moderate (n = 14), severe (n = 13) and critical (n =

24) disease from the first Hopital Cochin cohort. Interferon-stimulated gene (ISG) score (6 gene score) correlated with IFN α levels measured by (d) Simoa IFN α 2 (e) Simoa multi IFN α subtypes or (f) Luminex; n = 62. IFN activity (IU/mL) correlated with IFN α levels measured by (g) Simoa IFN α 2 (h) Simoa multi IFN α subtypes or (i) Luminex IFN α 2; n = 62. (j) IFN α 2, (k) multi IFN α subtypes (= equivalent IFN α 17) were measured by Simoa digital Elisa or (l) IFN α 2 by Luminex in patients with mild-to-moderate (n = 35), severe (n = 32) and critical (n = 22) disease from the second Hopital Cochin cohort. Lines indicate median values. P values were determined by multimodal regression models incorporating age and sex. Rs represents the Spearman coefficient. Healthy control = black, moderate COVID-19 patients = blue, severe COVID-19 patients = purple and critical COVID19 patients = red. *P < 0.05; **P < 0.01; ***P < 0.001.

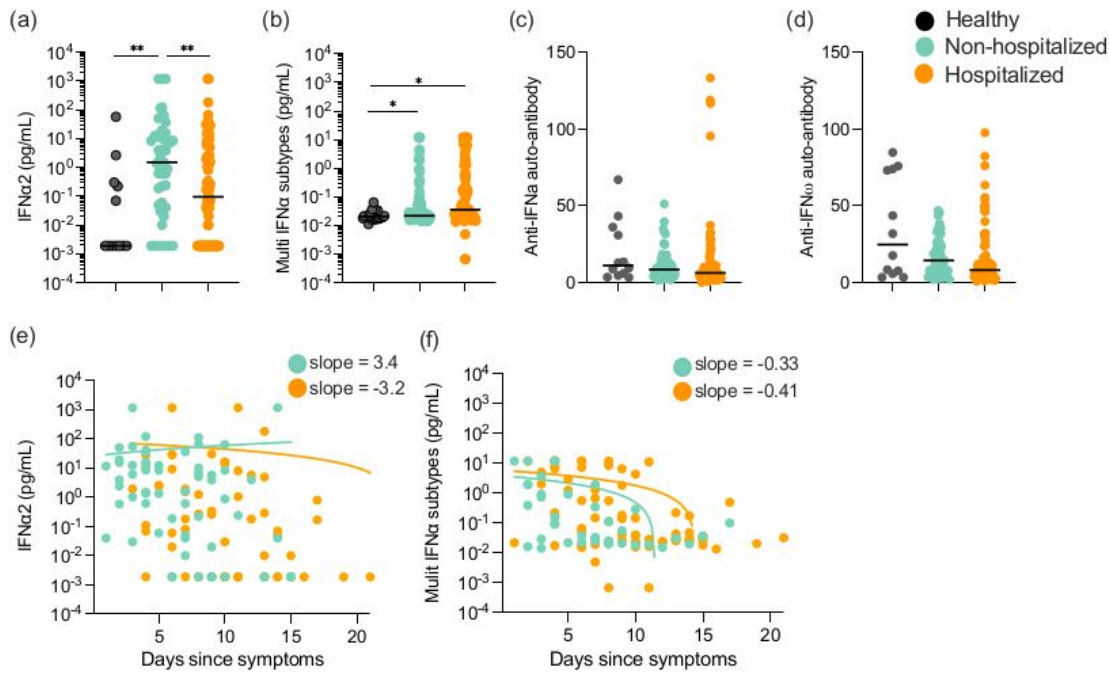


Figure 2

Figure 2

Plasma IFN α is consistently reduced in hospitalized patients independent of neutralizing auto-antibodies. (a) IFN α 2 and (b) multi IFN α subtypes (= equivalent IFN α 17) measured by digital ELISA Simoa in healthy controls (n = 12 donors), non-hospitalized (n = 46), or hospitalized (n = 80) COVID-19 patients of the St James Hospital cohort. (c) Anti-IFN α and (d) anti-IFN ω auto-antibodies in plasma of these healthy controls and COVID-19 patients. (e) IFN α 2 and (f) multi IFN α subtypes cytokine levels as a function of the

number of days post symptoms, with regression lines per COVID-19 patient groups shown. P values were determined by a multimodal regression models incorporating age and sex. Rs represents the Spearman coefficient. Lines indicate the median values. Healthy control = black, nonhospitalized COVID-19 patients = green and hospitalized COVID-19 patients = orange. *P < 0.05; **P < 0.01.

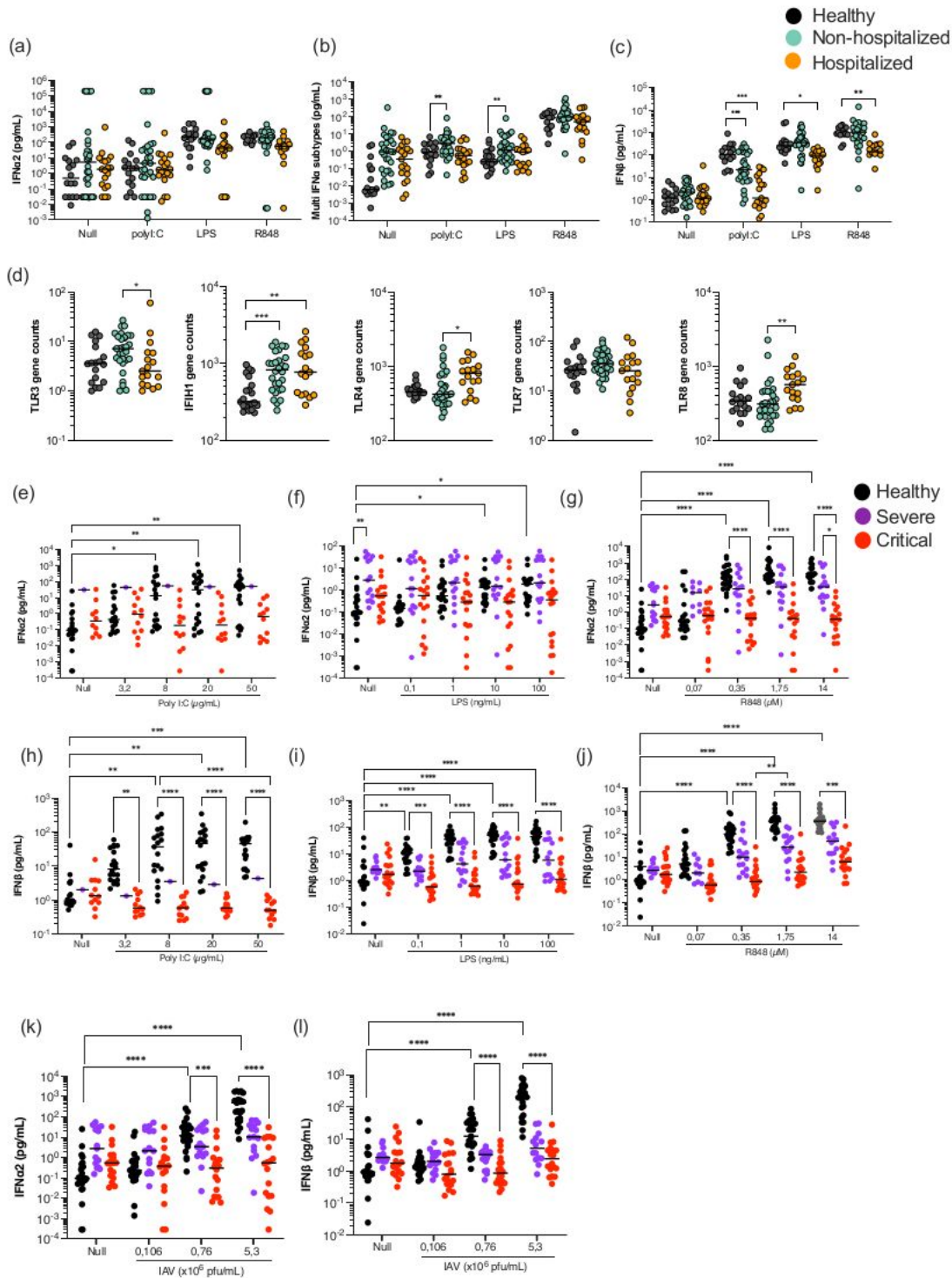


Figure 3

Figure 3

Induction of IFN-I response is perturbed in hospitalized patients. (a) IFN α 2, (b) pan-IFN α and (c) IFN β were measured by digital ELISA in healthy controls (n=19), nonhospitalized (n=27) and hospitalized (n=17) COVID-19 patients after 22h of whole blood stimulation with Poly:IC, LPS and R848. (d) mRNA of TLR3/4/7/8 and IFIH1 whole blood gene expression in healthy controls, non-hospitalized and hospitalized COVID-19 patients. IFN α 2 (e, f, g, k) and IFN β (h, i, j, l) responses in healthy donors (n=24), severe (n=11) and critical (n=20) COVID-19 patients after variable dose stimulation with Poly:IC (e, h), LPS (f, i), R848 (g, j) and influenza virus (k, l). Black lines represent the medians. P values were determined either by multimodal regression models incorporating age and sex, or by Kruskal–Wallis test followed by Dunn’s post hoc test for multiple comparisons. Healthy controls = black, non-hospitalized COVID-19 patients = green and hospitalized COVID-19 patients = orange, severe = purple and critical patients = red. *P < 0.05; **P < 0.01; ***P < 0.001; ****P < 0.0001.

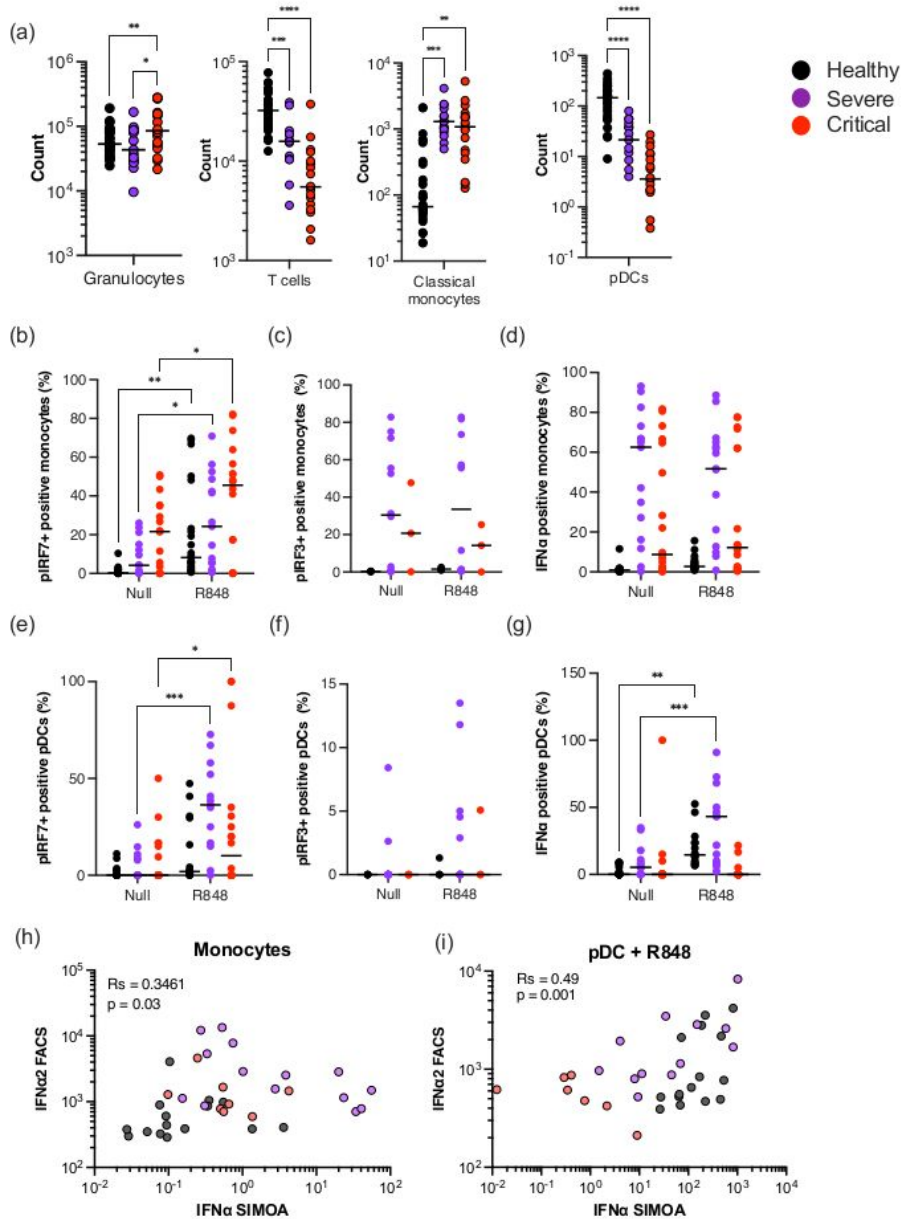


Figure 4

Figure 4

Perturbed intracellular IFN-I responses in COVID-19 patients. (a) Counts of granulocytes, T cells, classical monocytes, and pDCs in the blood of healthy controls (n=29), severe (n=11) and critical (n=20) COVID-19 patients. Percentages of (b, e) phosphorylated IRF7, (c, f) phosphorylated IRF3, or (d, g) intracellular IFN α positive monocytes (b, c, d) and pDCs (e, f, g) in the blood of healthy controls, severe and critical COVID-19 patients in the absence of stimulation of after overnight stimulation with R848. Correlation of

intracellular IFN α 2 measured by flow cytometry with plasma IFN α 2 levels measured by Simoa in (h) monocytes without stimulation or in (i) pDCs after R848 stimulation. P values were determined by Kruskal–Wallis test followed by Dunn’s post hoc test for multiple comparisons. *P < 0.05; **P < 0.01; ***P < 0.001; ****P < 0.0001.

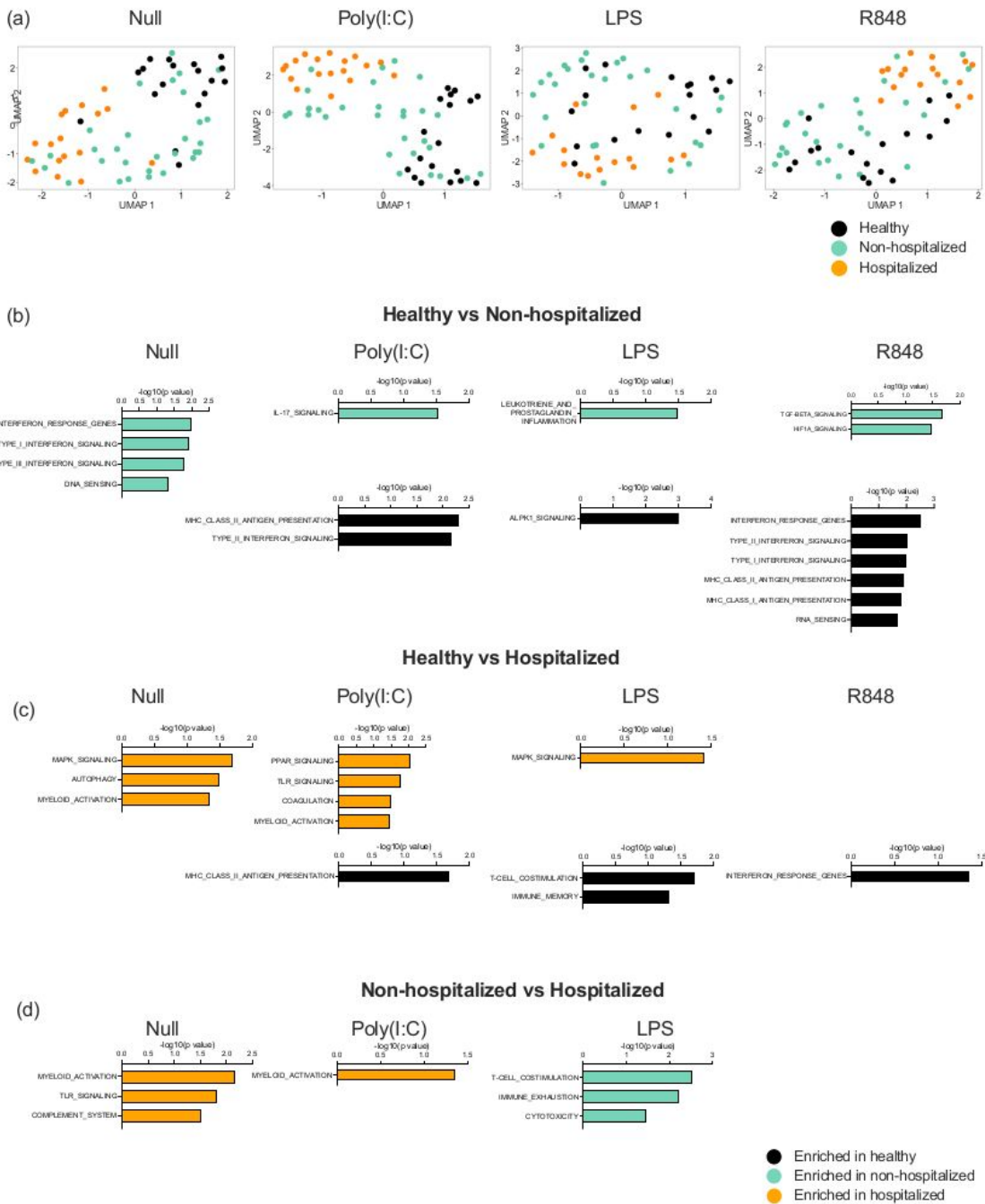


Figure 5

Figure 5

Induced gene expression differences in mild and hospitalized Covid-19 patients. (a) UMAP plots of Nanostring gene expression in the Null control, and after whole blood stimulation with Poly:IC, LPS, and R848. Gene expression pathways enriched in healthy donors (black, n=19), mild non-hospitalized COVID-19 patients (green, n=27), or hospitalized COVID-19 (orange, n=17) patients after comparisons between (b) healthy and mild, (c) healthy and hospitalized, (d) mild and hospitalized, after whole blood stimulation with Poly:IC, LPS, and R848.

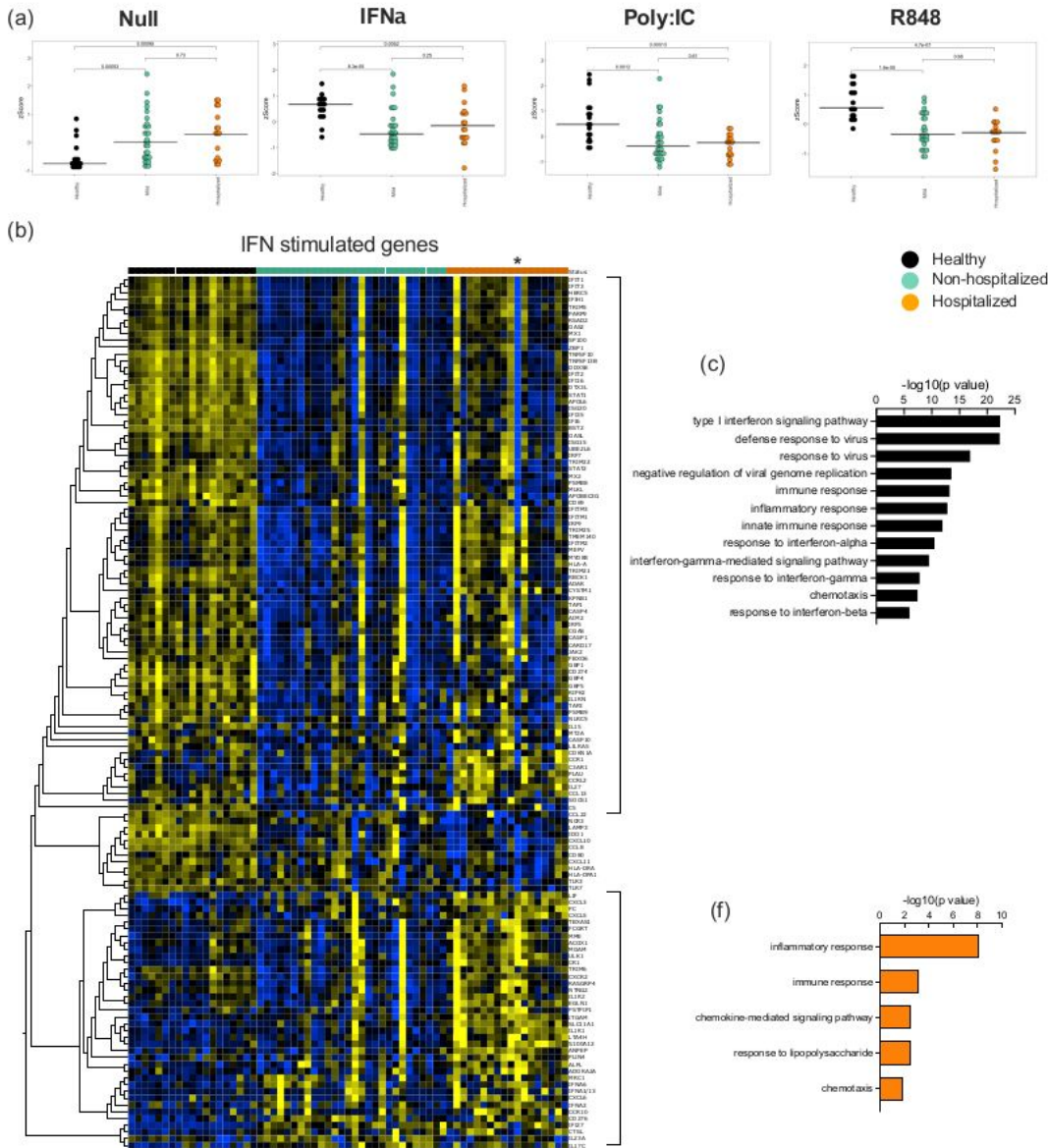


Figure 6

Figure 6

Downstream signaling response to IFN α is perturbed in hospitalized patients. (a) Type I interferon gene signature (ISG) score calculated from Nanostring data in healthy controls (black, n=19), mild COVID-19 patients (green, n=27), and hospitalized COVID-19 patients (orange, n=17) in the Null control, and after stimulation with IFN α , Poly:IC, and R848. (b) Heat map of all IFN stimulated genes identified from Nanostring data in healthy controls (black), mild COVID-19 patients (green), and hospitalized COVID-19 patients (orange). Pathways identified to be enriched after IFN α stimulation in (c) healthy donors and (f) hospitalized COVID-19 patients. Nanostring gene expression of (d) MX1, (e) TLR3 and TLR7, and (g) IL1R1 in whole blood of healthy controls (black), mild COVID-19 patients (green), and hospitalized COVID-19 patients (orange). Black lines represent the medians. P values were determined with the Kruskal–Wallis test followed by Dunn’s post hoc test for multiple comparisons. *P < 0.05; **P < 0.01; ***P < 0.001; ****P < 0.0001.

Supplementary Files

This is a list of supplementary files associated with this preprint. Click to download.

- [SmithetalSupplementalTablesS1.xlsx](#)
- [SmithetalSupplementalTablesS2.xlsx](#)
- [SmithetalSupplementalTablesS3.xlsx](#)
- [SmithetalSupplementalTablesS5.xlsx](#)
- [SmithetalSupplementalTablesS6.xlsx](#)
- [SmithetalSupplementalTablesS7.xlsx](#)
- [fs1.jpg](#)
- [SmithetalSupplementalTablesS4.xlsx](#)
- [fs2.jpg](#)
- [fs3.jpg](#)
- [fs4.jpg](#)